IMPROVING VISUALIZATION OF THREE-DIMENSIONAL ANEURYSM FEATURES VIA SEGMENTATION WITH UPSAMPLED RESOLUTION AND GRADIENT ENHANCEMENT (SURGE)*

Daniel E. MacDonald[1], Nicole M. Cancelliere[2], Arianna Rustici[2], Vitor M. Pereira[2, 3], and David A. Steinman[1]

[1]Biomedical Simulation Lab, Department of Mechanical & Industrial Engineering
University of Toronto, Toronto, Ontario, Canada
[2]Department of Neurosurgery, St Michael's Hospital, Toronto, Ontario, Canada
[3]Departments of Medical Imaging and Surgery
University of Toronto, Toronto, Ontario, Canada

ABSTRACT

Background: Intracranial aneurysm neck width tends to be overestimated when measured with three-dimensional rotational angiography (3DRA) compared with two-dimensional digital subtraction angiography (2D-DSA), owing to high curvature at the neck. This may affect morphological and hemodynamic analysis in support of treatment planning. We present and validate a method for extracting high curvature features, such as aneurysm ostia, during segmentation of 3DRA images.

Methods In our novel SURGE (segmentation with upsampled resolution and gradient enhancement) approach, the gradient of an upsampled image is sharpened before gradient-based watershed segmentation. Neck measurements were performed for both standard and SURGE segmentations of 3DRA for 60 consecutive patients and compared with those from 2D-DSA. Those segmentations were also qualitatively compared for surface topology and morphology.

Results Compared with the standard watershed method, SURGE reduced neck measurement error relative to 2D-DSA by >60%: median error was 0.49 mm versus 0.17 mm for SURGE, which is less than the average pixel resolution (∼0.33 mm) of the 3DRA dataset. SURGE reduced neck width overestimations >1 mm from 13/60 to 5/60 cases. Relative to 2D-DSA, standard segmentations were overestimated by 16% and 93% at median and 95th percentiles, respectively, compared with only 6% and 37%, respectively, for SURGE.

Conclusion SURGE provides operators with high-level control of the image gradient, allowing recovery of high- curvature features such as aneurysm ostia from 3DRA where conventional algorithms may fail. Compared with standard segmentation and tedious manual editing, SURGE provides a faster, easier, and more objective method for assessing aneurysm ostia and morphology.

What is already known on this topic
⇒ Intracranial aneurysm necks tend to be overestimated when measured from 3D imaging, which may impact treatment planning and morphological analysis.

What this study adds
⇒ We quantified the prevalence of neck overestimation in a consecutive sample of 60 cases, and introduced a new method for reducing errors associated with overestimation: SURGE—segmentation with upsampled resolution and gradient enhancement.

*Citation: This article has been accepted for publication in *J Neurointerv Surg* 15:760-765 (2023) following peer review, and the Version of Record can be accessed online at http://dx.doi.org/10.1136/neurintsurg-2022-018912.

How this study might affect research, practice and/or policy
⇒ The proposed SURGE method enables better 3D characterization of aneurysm morphology and reduces extreme neck overestimations that might skew cohort studies.

1 Introduction

Two-dimensional digital subtraction angiography (2D-DSA) is considered to be the gold standard imaging modality for intracranial aneurysm assessment due to its superior image and contrast resolution compared with the less invasive CT angiography (CTA) and magnetic resonance angiography (MRA) [1]. Three-dimensional rotational angiography (3DRA) imaging has become common for cerebral angiography, allowing clinicians to view 3D aneurysm features that may be missed on 2D imaging, such as aneurysm sac blebs and parent vessel fenestrations. 3DRA is a useful tool for modern procedure planning including device sizing, which is highly dependent on vessel and aneurysm measurements.

Despite 3DRA having higher spatial resolution among intracranial vascular 3D imaging modalities, segmentation from 3DRA images is still challenging and may produce inconsistent measurements. In a comparison of 205 intracranial aneurysms [2], 3DRA was shown to systematically overestimate neck width compared with 2D-DSA, which has implications for treatment decisions, device sizing, and predicted outcomes of endovascular therapy. Such overestimation may also have an impact on research of rupture mechanics and risk assessment: in a study of n=20 aneurysms, researchers manually edited the overestimated 3DRA segmentations (8/20) to match 2D-DSA imaging and showed non-negligible changes in inflow jet dynamics and wall shear stresses using computational fluid dynamics (CFD). In an international aneurysm segmentation challenge, participating teams consistently over-estimated neck width in one case; only one team accurately recovered the neck through empirical inspection and manual editing of the segmented model, involving a reported editing time of 26 hours [3]. In a more recent international aneurysm segmentation challenge highlighting deep-learning techniques, the neck was cited as the most common and substantial region of error among top submitted solutions [4].

Overestimation of neck width may occur when the sac is in close proximity to adjacent arteries, resulting in blurred regions between the adjacent structures. In this paper, we show how a conventional gradient-based image segmentation pipeline can be modified to improve segmentation, with an emphasis on improving ostium measurements from 3DRA. We applied this novel method, SURGE (segmentation with upsampled resolution and gradient enhancement), to 60 consecutive cases and compared ostium measurements with 2D-DSA and conventional watershed segmentation. We tested whether each of these measures was statistically different, and provided concrete examples to highlight representative changes.

2 Methods

2.1 SURGE pipeline

Our proposed segmentation pipeline is based on the watershed method, which considers the image gradient as a topographic map of peaks and basins, whereby "flooding" the map from user-defined marker-points can be used to identify disconnected regions [5]. We modify the conventional watershed pipeline in two ways: (1) before computing the gradient, we upsample the image using bicubic interpolation, and; (2) we sharpen the gradient image using the Difference-of-Gaussians feature-enhancement method using blurring kernels $\alpha_1 = 0$ and $\alpha_2 = 1$ [6]. By upsampling the image, we improve spatial resolution at the cost of reducing contrast resolution. The Difference-of-Gaussians method sharpens gradient peaks and erodes regions between adjacent peaks. Image sharpening alone may not separate adjacent vessels because it is constrained by the image resolution; by upsampling first, we can identify adjacent peaks with sub-pixel resolution. This process, illustrated in Fig. 1, has the effect of amplifying the lumen-wall boundary while attenuating regions between adjacent vessels.

The SURGE pipeline thus has two operator-defined parameters: upsampling rate (UR, the factor by which resolution is increased) and gradient enhancement (GE, which blends the standard and sharpened gradient images). Using the sharpened image alone (GE = 1) may undesirably amplify noise or worsen regions of uneven contrast, so we use a default value of GE = 0.5 in this study to provide moderate enhancement.

The standard and SURGE watershed segmentation pipelines are implemented in Python 3.8 using numpy [7], scikit-image [8], PyVista [9], and the Visualization Toolkit (VTK) [10], i.e. all open-source toolkits to allow other groups to easily implement/replicate SURGE. Surfaces are generated from the segmented image using VTK's vtkMarchingCubes filter and smoothed using the volume-preserving vtkWindowedSincPolyDataFilter.

Fig. 1 compares a standard watershed method pipeline with the SURGE method using case E from the Multiple Aneurysms Anatomy Challenge 2018 as an example [3]. Fig. 1B shows the gradient of the original image; though the

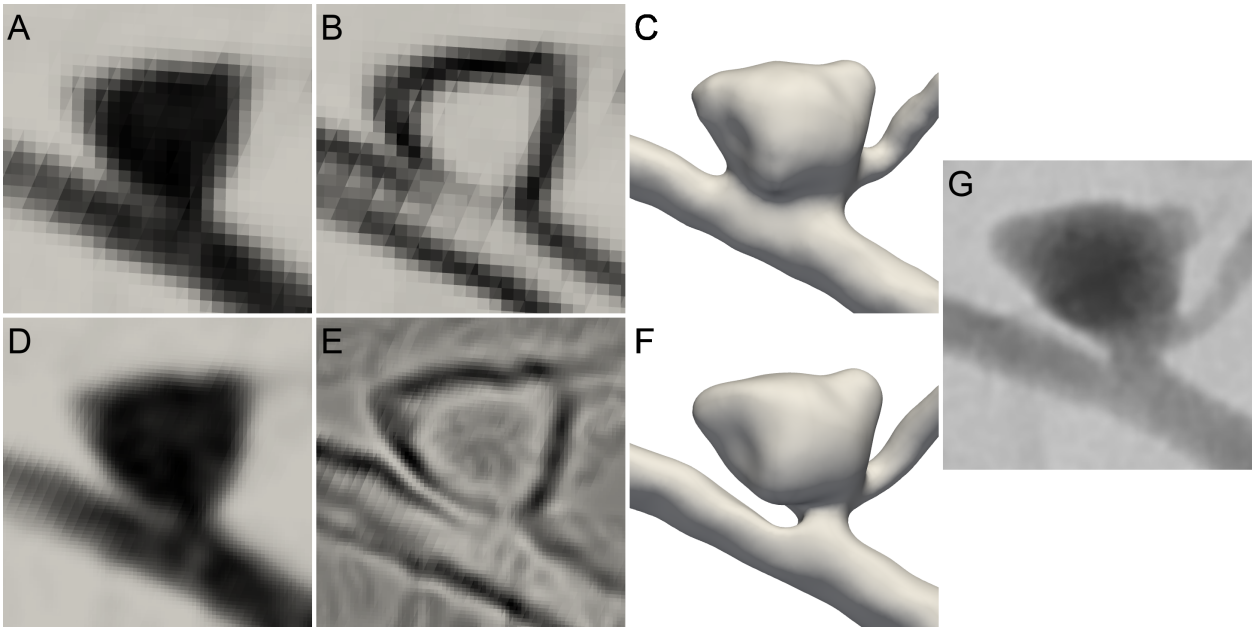

Figure 1: Comparison of standard watershed method pipeline (A-C) versus SURGE pipeline (D-F), illustrated using a 2D slice through the neck of case E from the Multiple Aneurysms Anatomy Challenge 2018.3 (A) Grayscale intensity in its original resolution; (B) gradient of the original-resolution image; (C) surface contour using standard watershed method; (D) upsampled grayscale intensity using bicubic interpolation (UR=3); (E) gradient of upsampled grayscale intensity with gradient enhancement using the Difference of Gaussians filter (GE=0.7); (F) surface contour using SURGE watershed method; (G) 2D-DSA projection of ostium. The values of UR and GE were iteratively chosen by the operator beginning with UR=2 and GE=0.5 until the surface matched the gradient. The total processing time to generate both the standard and SURGE surfaces (comprising ROI selection, marker selection, iterative choice of parameters, and basic surface reconstruction) was 1 min 46 s for an ROI of size 14x10x10 mm^3. 2D-DSA, two-dimensional digital subtraction angiography; GE, gradient enhancement; ROI, region of interest; SURGE, segmentation with upsampled resolution and gradient enhancement; UR, upsampling rate.

neck outline is visible to the eye, it is difficult to capture algorithmically due to non-uniform contrast and low spatial resolution. Using bicubic upsampling (Fig. 1D), the resolution of the original image is enhanced. Fig. 1E shows the gradient of this upsampled image with subtle sharpening to enhance gradient peaks and attenuate regions between adjacent vessels. Comparing the SURGE gradient (Fig. 1E) with the gradient of the original image (Fig. 1B), the apparent image quality is improved, though background noise is slightly amplified. Comparing the standard surface (Fig. 1C) with the SURGE surface (Fig. 1F), the latter is observed to better align with the contour of maximal gradient and with the 2D-DSA projection (Fig. 1G).

2.2 Patients

Patients in this series received aneurysm treatment including coiling and/or placement of a stent or balloon angioplasty during the period of April 2019—October 2020 and received both 2D-DSA and 3DRA imaging during treatment. Cases were retrospectively collected from the institution's PACS and analyzed following Institutional Research Ethics Board approval. We excluded cases that were previously treated and those in which a good working projection of the aneurysm neck was unavailable.

2.3 Angiographic technique

Catheter-based angiograms were performed as per hospital standard of care. Femoral or radial access was obtained and a 5F diagnostic or 6F distal access catheter was navigated over a wire, +/- microcatheter, into the internal carotid or vertebral artery. 2D-DSA imaging was acquired at a rate of 2 frames per second using a calibrated flat-detector biplane DSA system (Allura Clarity, Philips Healthcare, Best, NL) and an 8 mL bolus of iodinated contrast media Omnipaque/iohexol (300 mgI/mL) injected at a rate of 4 cc/s. Selected working projection views were optimized to see the aneurysm neck in profile. The object-to-detector distance was minimized to reduce the effect of magnification.

The smallest field of view to include all pertinent anatomy was used, most often 15 cm (i.e. the smallest allowable size on the system) but sometimes up to 22 cm, and the image matrix size was 10242.

3DRA images were acquired using a 3 cc/s injection of Omnipaque/iohexol (300 mgI/mL) over a 4.07 s acquisition (30 frames per second), with a 3 s delay (24 cc total injection) to allow for sufficient contrast mixing and fully opacified vessels during the entire length of the acquisition (122 frames total). The 3DRA volumes were reconstructed using the Philips interventional 3D workstation's (Xtravision) standard reconstruction algorithm which uses a normal reconstruction kernel with 100% magnification and a matrix of 384 pixels^3, producing DICOM images with a median isotropic resolution of 0.33 mm (interquartile range = 0.11, range = 0.23-0.63).

2.4 Measurement of neck width

Neck widths were measured by two raters (a neuroradiologist and an experienced research technologist) from 2D-DSA images by first calibrating to the intermediate catheter or microcatheter to avoid undue magnification of off-axis objects. Measurements were made using measurement tools provided on our hospital PACS (Carestream Client; version 12.1.6.1005).

For each patient's 3DRA volume, we extracted an ROI containing the aneurysm (average size = (12 x 12 x 12) mm3) and generated standard and SURGE segmentations while blinded to 2D-DSA images and measurements. The watershed marker-points were consistent between each pair of segmentations. To measure neck width for the standard and SURGE surfaces, an orthographic camera view was chosen to match the 2D-DSA working projection. The ostium of each surface was then measured from the chosen projection using a tool built with Python 3.8 using PyVista[9] and VTK [10], taking care to match the neck plane location independently used for 2D-DSA.

2.5 Statistical analysis

We hypothesized that measurements from SURGE would be statistically different compared with standard watershed segmentation, and that SURGE measurements would be closer to 2D-DSA compared with standard measurements. These three neck measurements were all found to follow non-normal distributions using the Shapiro-Wilk test, so we tested each pair of measurements (standard vs SURGE, standard vs 2D-DSA, SURGE vs 2D-DSA) for statistical differences using the two-sided Wilcoxon Signed Rank test. For each of the two 3D segmentation methods, we also tested for differences in error between sidewall and bifurcation aneurysms using the Mann-Whitney U test. Inter-rater agreement for the 2D-DSA neck widths was calculated as the intraclass correlation coefficient.

3 Results

Sixty aneurysms were retrospectively included in our study, including 38 bifurcation aneurysms and 22 sidewall aneurysms. The median aneurysm size was 4.82 mm (range 1.58—13.38 mm) with median neck size 3.35 mm (95% CI = 2.78—3.70, range 0.88—7.61 mm). The most common aneurysm location was the anterior cerebral artery (ACA: n = 26, 43%) followed by internal carotid artery (ICA: n = 25, 42%), vertebrobasilar (n = 7, 12%) and middle cerebral artery (MCA: n = 2, 3%). Additional cohort information is included as a data supplement.

Inter-rater differences in neck width from 2D-DSA were not significantly different from zero ($p = 0.27$), and with an intra-class correlation coefficient >0.98, so we used the average of the two reads for all comparison to 3D neck measurements. Standard and SURGE measurements differed significantly from each other ($p < .0001$) (Table 1), and each of these measurements also differed significantly from 2D-DSA measurements, albeit SURGE to a lesser degree (standard vs 2D: $p < .0001$, SURGE vs 2D: $p = 0.002$). For both standard and SURGE neck measurements, median error was greater in bifurcation aneurysms, but not significantly (see Table 2). All individual neck measurements are included in the data supplement.

Both standard and SURGE segmentations generally overestimated neck width compared to 2D-DSA; the distribution of these errors is shown in Fig. 2a. For standard watershed, median error relative to 2D-DSA was 0.49 mm for standard, significantly higher ($p < .0001$ using a one-sided Wilcoxon Signed Rank test) than the 0.17 mm for SURGE. Note that the latter is less than the typical resolution of the reconstructed 3DRA volumes ($\sim$0.33 mm), suggesting that median SURGE errors are on the order of single pixels. Both error distributions show a long tail, with 75th and 95th percentile errors of 0.95 and 2.11 mm for standard, and 0.44 and 1.08 mm for SURGE. Using 1 mm (i.e., >3 pixels, or $>30\%$ error considering the median neck width of 3.35 mm in our cohort) as a somewhat arbitrary threshold for non-negligible overestimation relative to 2D-DSA, neck widths for 13/60 cases were overestimated by standard segmentation, but only 5/60 cases by SURGE. Note also that, for both standard and SURGE, any neck underestimations relative to 2D-DSA were always $<= 0.75$ mm.

Table 1: Descriptive statistics and results of hypothesis tests comparing measurement of aneurysm neck width from standard watershed segmentation, SURGE, and 2D-DSA

		Error relative to 2D-DSA		vs. SURGE		vs. 2D-DSA	
	Median [mm]	Median [mm]	Median [%]	W[a]	p-value	W[a]	p-value
Standard	3.83 (3.21—4.35)	.49 (.32—.62)	16 (10—24)	21	.0001	150	.0001
SURGE	3.43 (3.00—3.81)	.17 (.08—.32)	6 (3—9)	-	-	491	0.002

Error relative to 2D-DSA was calculated for standard and SURGE in millimetres (indicated as Median (mm), as in Fig. 2A), and as a percentage error (indicated as Median (%), as in Fig. 2B).
Statistical differences were tested between paired measurements using the Wilcoxon signed-rank test. The presented errors consider only the width of the neck; measures such as volume, sac diameter, or merging artifacts shown in Fig. 3A were not quantified.

Table 2: Comparison of measurement errors for bifurcation vs. sidewall aneurysms using standard and SURGE segmentation methods relative to 2D-DSA

	Bifurcation median (mm)	Sidewall median (mm)	U[a]	p-value
Standard	0.54 (0.36-0.7)	0.38 (0.17-0.68)	470	0.43
SURGE	0.19 (0.035-0.34)	0.11 (-0.048-0.38)	447	0.66

Note: value ranges in round brackets indicate 95% confidence intervals generated using the percentile bootstrap method with 5000 iterations.
[a]Test statistic for the Mann-Whitney U test

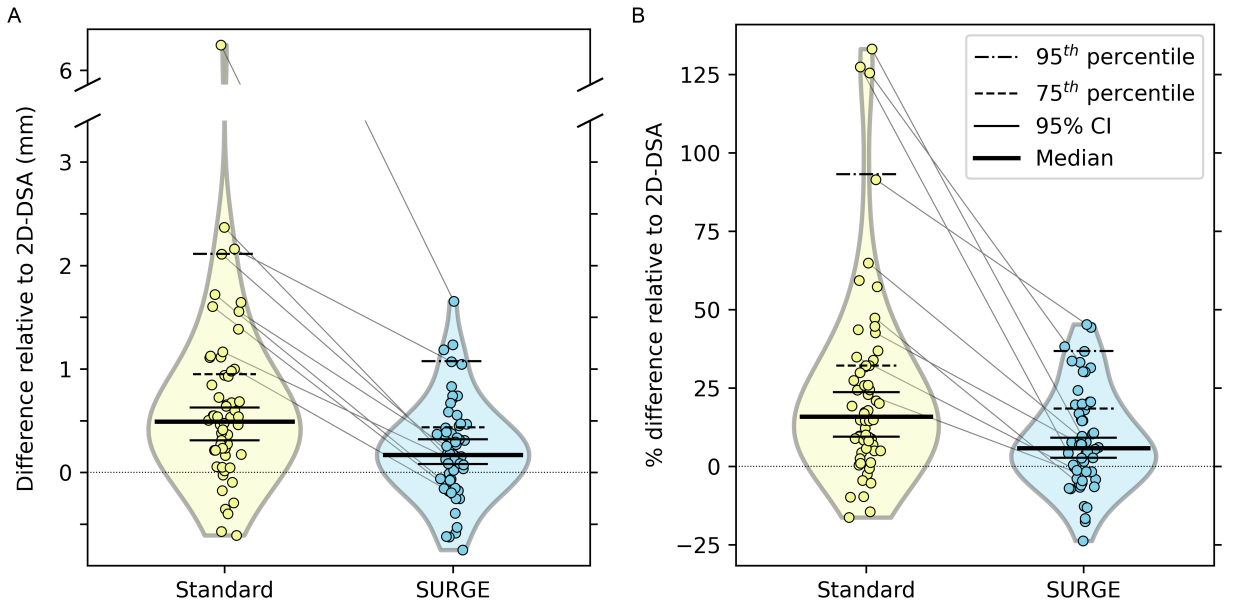

Figure 2: Errors in neck width relative to gold standard 2D-DSA measurement. Violin plots are used to show the distribution of errors. (A) Difference in neck width (millimetres) relative to 2D-DSA measurements. The horizontal bars indicate median and 95% CI (see Table 1). Where measurements between standard and SURGE differ by >1 mm, a sloped line is used to highlight the differences. (B) Percentage error relative to 2D-DSA measurements. Horizontal bars indicate median and 95% CI (see Table 1). Sloped lines indicate cases demonstrating a change >25% between 3D measurement methods. 2D-DSA, two-dimensional digital subtraction angiography; 3D, three-dimensional; SURGE, segmentation with upsampled resolution and gradient enhancement.

A potential outlier is observed above the split y-axis of Fig. 2a, for which standard watershed considerably overestimates neck width (standard = 11.22 mm, SURGE = 6.63 mm, 2D-DSA = 4.98 mm); this case was located at the ACA bifurcation and had a very wide sac (>13 mm) that fully merged with an adjacent vessel, resulting in an abnormally high absolute difference (>6 mm, which was greater than the cohort median sac size). To ensure our results were not favorably skewed by this datapoint, we reran all statistical tests with this case omitted, and the results of all tests were unchanged.

Fig. 2b shows the percentage-difference between 3D segmentation measurements and 2D-DSA. Using standard watershed, 21/60 cases exhibit error greater than 25% compared with 9/60 using SURGE, with median error of 16% and 6% respectively (see Table 1). As in Fig. 2a, the error distribution of the standard measurements shows a long tail, with 75th and 95th percentile errors of 32% and 93%. SURGE reduced the 75th and 95th percentile errors to 18% and 37%.

Fig. 3 shows representative cases that demonstrated varying degrees of difference between standard and SURGE segmentations, and compares them with the gold-standard 2D-DSA. Case A demonstrates a reduction in neck width in agreement with the gradient and 2D-DSA images and shows improved segmentation of nearby small branches and blebs. In cases B and C, the standard method merges a nearby small branch with the parent artery, while SURGE separates the branch resulting in a concavity between the branch and the parent. These concavities are present in the image gradient and show greater agreement with 2D-DSA. Case D demonstrates a 2.3 mm change between standard and SURGE. The gradient image shows that the small neck apparent in the 2D-DSA image is captured in the 3DRA volume, but that the gradient is weak near the neck. In case E, SURGE results in a moderate reduction in neck width, improving agreement with the 2D-DSA profile. A fenestration is observed in the 2D-DSA projection, but this feature is not captured by either standard or SURGE.

The median processing time for SURGE, including user ROI selection, marker selection, iterative choice of UR and GE, and basic surface construction was 1 min 36 s on a consumer laptop, with choice of GE and marker selection requiring the bulk of this time.

4 Discussion

This work demonstrates a principled method for overcoming ostium overestimation and recovering resolution of aneurysm sac features. We have shown that, by interpolating and enhancing these gradients prior to gradient-based segmentation, vessel borders with high curvature (such as aneurysm ostia) can be better delineated. This approach avoids the need for manually estimating and/or editing the ostium contour, thus saving operator time and effort.

Compared to the standard watershed method, SURGE reduced neck measurement error relative to 2D-DSA by >60% (from 0.49 to 0.17 mm) and the cohort median error was less than the average pixel resolution (∼0.33 mm) of the 3DRA dataset. As observed in Fig. 2a, SURGE effectively targets many "extreme" errors resulting from standard gradient-based segmentation, reducing the range and dispersion of errors. SURGE may therefore be especially useful for correcting such outlier cases that might otherwise skew cohort measurements, thus rendering neck/ostium measurement from 3DRA more reliable.

4.1 Relationship to previous work

Previous studies comparing neck width between 2D-DSA and 3DRA imaging have used threshold-based contours (which require subjective choice of threshold) [2] and gradient-based methods[11] to extract the lumen surface from the image. Research highlighting the issue of neck overestimation in 3D segmentation has been consistent over time [2, 3, 11, 12], but to our knowledge, no solutions have been proposed and tested for correcting ostium overestimation.

In principle, modern deep-learning methods may be capable of overcoming neck overestimation, but in practice, such methods usually rely on manually annotated data (which is both subjective and time-consuming to generate [3]) and once trained, provide little interpretability. The recent Cerebral Aneurysm Detection and Analysis challenge showcased some of these technical advancements [4], but neck and near-aneurysm errors were not systematically quantified; the authors did, however, indicate that the neck and aneurysm surface was the most common region of error among top-performing participants.

Furthermore, in any aneurysm image, the neck region represents only a tiny fraction of the image volume, and common metrics of segmentation performance (accuracy, Jaccard index, F1-score) would not differentially account for the relative importance of this region—in [4], the top reported Jaccard index of 0.92 indicates good segmentation broadly but does not convey the model performance for fine near-aneurysm features like neck width, bleb formation,

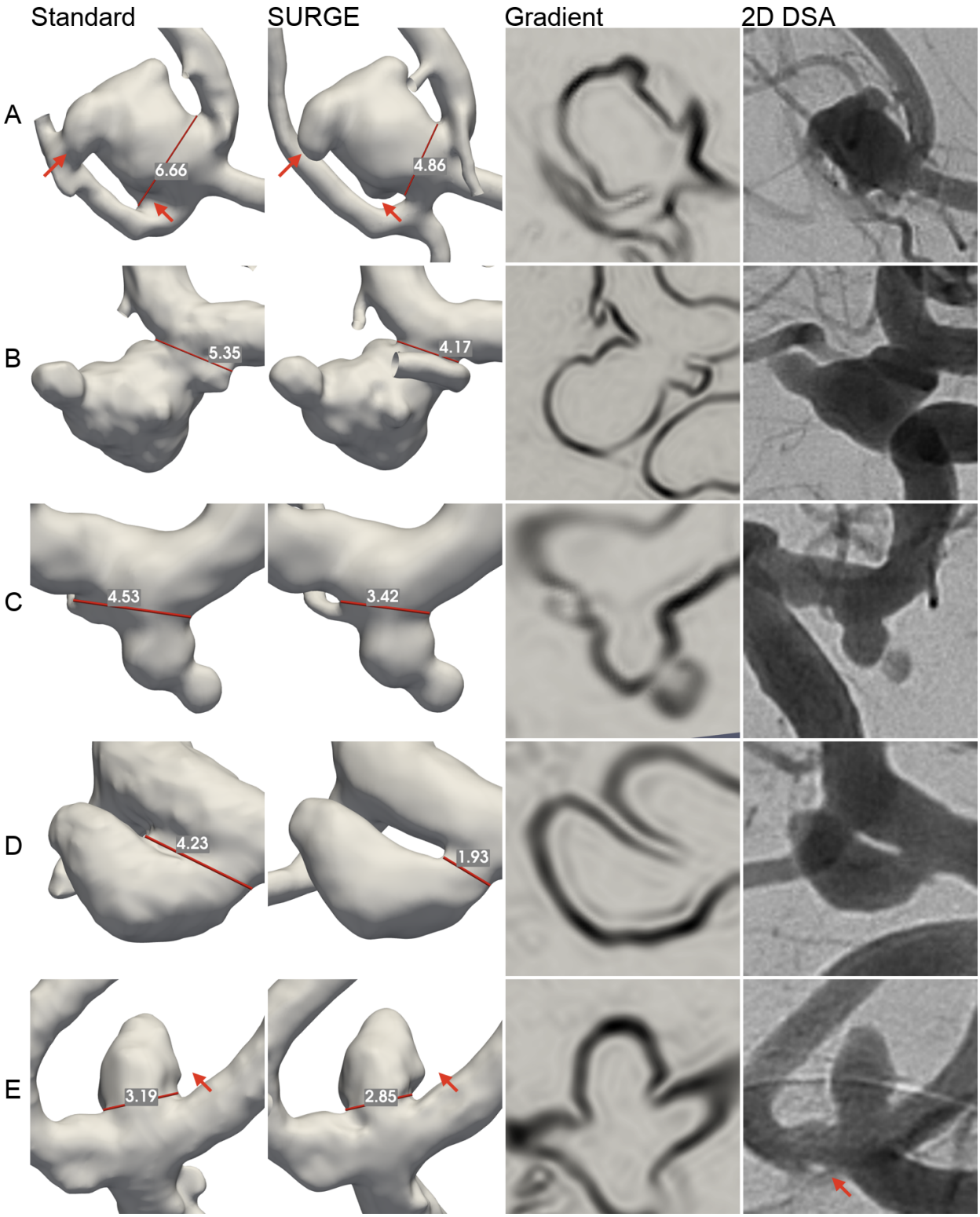

Figure 3: Visualization of ostium and sac changes between standard watershed and SURGE for five cases showing varying degrees of overestimation. 2D-DSA, two-dimensional digital subtraction angiography; SURGE, segmentation with upsampled resolution and gradient enhancement.

or the presence of small branches. These summary metrics should therefore be interpreted critically in the context of aneurysm treatment.

The interpretable gradient image presented herein (Fig. 1E) may be useful in this context for manually annotating data or assessing the quality of segmentations, as has been suggested previously for standard gradient images [13, 14]. In contrast to deep-learning methods that often provide opaque interpretability, our work encourages manual inspection of the gradient image, and especially of the upsampled gradient, for assessing segmentation quality; for example, the lumen boundary is clearer in Fig. 1E compared with Fig. 1A, and we confirm that our segmentation matches Fig. 1E.

4.2 Clinical and clinical study implications

Our method for recovering blurred aneurysm features may improve aneurysm assessment, treatment approach and study of aneurysm growth and rupture. Generally speaking, aneurysms with narrower necks are safer to be coiled alone compared to wide-necked aneurysms [15], which may require support from an open-celled stent (i.e. stent-assisted coiling) or flow diverting stent. Intra-saccular device choice and sizing can also be positively influenced with more accurate and precise (i.e., reproducible) measurements. By way of illustration, using 2D-DSA, 15/60 cases in our cohort would be classified as wide-necked according to a simple 4-mm threshold [16]. Using standard segmentation, an additional 11 cases would have been classified as wide-necked, compared to only 5 using SURGE. Improved resolution of sac features could also help improve detection of aneurysm growth or sac changes on follow-up imaging for untreated patients that are being monitored, which have been shown to be correlated with a higher risk of rupture [17, 18]. In the future, we plan to assess our SURGE method for less-invasive imaging modalities, as often patients are initially assessed or followed using CTA or MRA.

While some of the underlying blurring artifacts could in principle be mitigated by appropriate choice of reconstruction kernel and storage resolution at the time of imaging/reconstruction [19, 20], the reality is that raw 3DRA data or high-resolution reconstructions are often not saved to hospital picture archiving and communication systems (PACS), since this increases data storage requirements and may not be prospectively justified in routine clinical settings [19]. Thus, for retrospective studies, the reconstruction method may be out of control of researchers. Our approach, therefore, introduces the ability to retrospectively "restore", at least partially, already-reconstructed 3D image volumes saved to hospital PACS.

SURGE may also provide benefit for 3DRA volumes that were prospectively reconstructed at higher resolution or with different kernels, i.e., already effectively upsampled. For example, we applied SURGE to a reconstructed volume of case E from Fig. 3 (using resolution 0.12 mm vs. 0.33 mm) and were able to extract the fenestration observed in 2D-DSA, which still could not be extracted using standard watershed (Fig. 4). Extra caution must be exercised in the presence of nearby fenestrations when treatment includes balloon-assistance or stent placement. The ability of SURGE to fix artifacts relies on the scale of the pixel size relative to the features; in Fig. 3, the diameter of the fenestration relative to the pixel size is small, but increases with higher resolution reconstruction.

Finally, just as in any interpretable segmentation method (such as thresholding, level-set, or watershed methods), some iterative tuning of parameters by the operator may be required to achieve a satisfactory segmentation. A default value of UR = 2 was set for all cases, but UR = 3 was also used at operator discretion when overestimation or artifact was still suspected after applying UR = 2 (12/60 cases). A default value of GE = 0.5 was chosen in this study and operator choice fell within the range of 0.3 and 0.8 for all cases during initial segmentation. In some cases (for example case D of Fig. 3), simply using UR = 2 and GE = 0 resulted in improved segmentation, suggesting some extreme errors may be mitigated by upsampling alone.

4.3 Potential limitations

In this study, 2D-DSA is assumed to be the "ground-truth" standard of reference, and although it does provide higher spatial and contrast resolution than 3DRA, neck width measurements are not without uncertainty. In our study, each of the two raters used a single window/level setting for each case, which may affect the apparent neck width. As discussed in the Methods, these measurements were each calibrated to the intermediate catheter to reduce off-axis magnification effects, but each calibration may introduce variability to the 2D-DSA measurements. Previous studies have discussed the advantages (resolution) and limitations (occlusion and view angles) of 2D-DSA relative to 3DRA for tasks such as aneurysm detection or shape visualization [1, 21, 22]. For ostia with high eccentricity, a single projection may fail to capture the complex shape, and a single neck measurement may be misleading, so SURGE may help characterize and visualize these complex ostium shapes.

The described pipeline is of course limited by the quality of the original image, and will only fix potentially-recoverable partial volume effects. Where poor contrast-agent-mixing is present, for example in large aneurysms with regions of

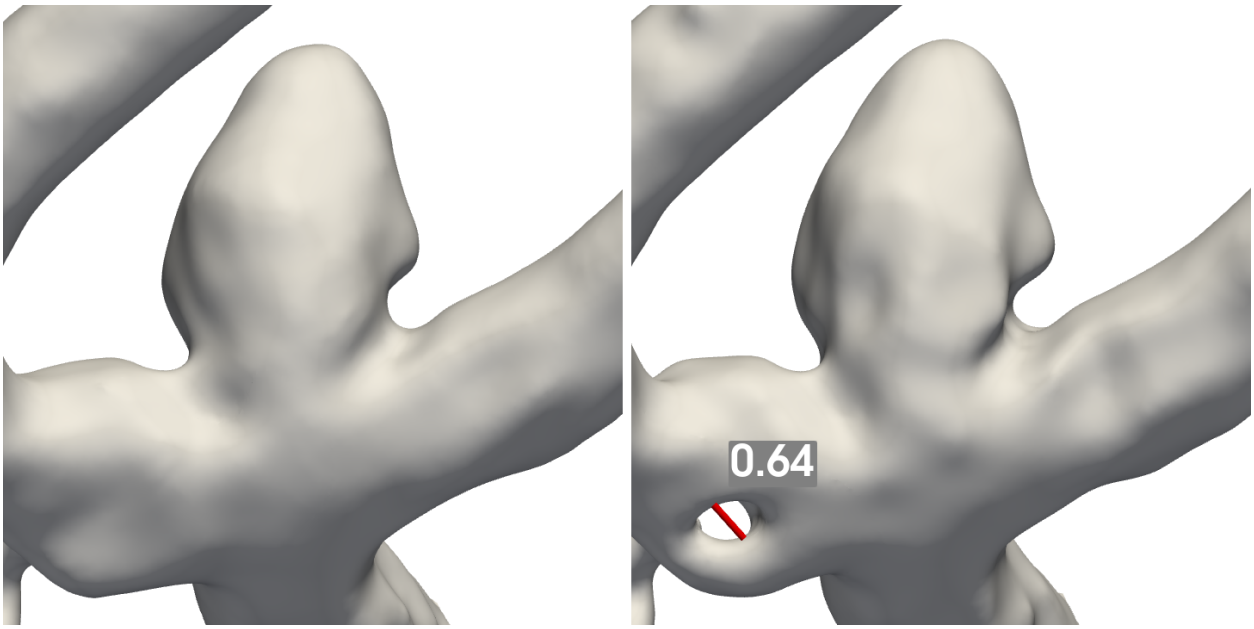

Figure 4: SURGE was applied to a high-resolution 3DRA reconstruction (pixel spacing = 0.12 mm) of case E from Fig. 3; SURGE (right) captures the fenestration where standard segmentation (left) still fails.

stagnant flow, artifacts may be amplified. SURGE also introduces further computational complexity to the segmentation pipeline due to the image upsampling step, but additional computation time is on the order of seconds for limited ROIs (i.e., focused on the sac). For larger ROIs, memory requirements (and computation time) will be more substantial, scaling proportionally to the image volume; e.g. a volume of 64^3 mm^3 will require 4^3 time more resources than a volume of size 16^3 mm^3. For larger ROIs including the full parent artery and daughter branches (e.g. for the purposes of CFD), segmentation time may be on the order of minutes to tens-of-minutes. It may be advantageous to selectively apply SURGE only on limited ROIs (i.e., the sac) and merge the output with a standard segmentation. Though we have indicated how SURGE may aid in patient assessment and follow-up, we have not shown that patient management would be different with the application of our SURGE pipeline. However, SURGE can reduce extreme mischaracterization of aneurysm ostia while improving shape characterization, which may be especially useful for tracking unruptured patient outcomes and for restoring already-reconstructed 3DRA volumes.

5 Conclusion

SURGE provides a method for recovery of high-curvature features such as aneurysm ostia during segmentation from 3DRA by using a straightforward image processing pipeline. It provides objective, high-level control of segmentation guided by image gradients and is easier and more efficient than manual editing. It can be implemented within standard gradient-based segmentation pipelines, and used selectively when desired or deemed necessary. Such may be the case for advanced morphological or patient-specific CFD analyses where errors in sac/ostium morphology may affect flow patterns or rupture risk assessment. In principle, SURGE is extendable to other modalities (CTA, MRA) and ultimately may help make less invasive 3D imaging more reliable for treatment planning where accurate neck/ostia measurements are crucial.

6 Acknowledgements

VMP acknowledges the generous support from Michael's Family; a JDMI/UHN Research Leadership Award; and the Schroeder Chair in Advanced Neurovascular Interventions. DEM acknowledges the generous support of an Ontario Graduate Scholarship and a Barbara & Frank Milligan Graduate Fellowship.

References

[1] W. van Rooij et al. "3D Rotational Angiography: The New Gold Standard in the Detection of Additional Intracranial Aneurysms". In: *American Journal of Neuroradiology* 29.5 (May 2008), pp. 976–979. DOI: 10.3174/ajnr.A0964.

[2] W. Brinjikji et al. "Comparison of 2D Digital Subtraction Angiography and 3D Rotational Angiography in the Evaluation of Dome-to-Neck Ratio". In: *American Journal of Neuroradiology* 30.4 (Apr. 2009), pp. 831–834. DOI: 10.3174/ajnr.A1444.

[3] P. Berg et al. "Multiple Aneurysms AnaTomy CHallenge 2018 (MATCH): Phase I: Segmentation". In: *Cardiovascular Engineering and Technology* 9.4 (Dec. 2018), pp. 565–581. DOI: 10.1007/s13239-018-00376-0.

[4] M. Ivantsits et al. "Detection and analysis of cerebral aneurysms based on X-ray rotational angiography - the CADA 2020 challenge". In: *Medical Image Analysis* 77 (Apr. 2022), p. 102333. DOI: 10.1016/j.media.2021.102333.

[5] S. Beucher and F. Meyer. "The Morphological Approach to Segmentation: The Watershed Transformation". In: *Mathematical Morphology in Image Processing*. Ed. by E. R. Dougherty. 1st ed. CRC Press, Oct. 2018, pp. 433–481. DOI: 10.1201/9781482277234-12. URL: https://www.taylorfrancis.com/books/9781482277234/chapters/10.1201/9781482277234-12 (visited on 05/10/2022).

[6] R. Szeliski. *Computer Vision: Algorithms and Applications, 2nd Edition*. URL: http://szeliski.org/Book/.

[7] C. R. Harris et al. "Array programming with NumPy". In: *Nature* 585.7825 (Sept. 2020), pp. 357–362. DOI: 10.1038/s41586-020-2649-2.

[8] S. van der Walt et al. "scikit-image: image processing in Python". In: *PeerJ* 2 (June 2014), e453. DOI: 10.7717/peerj.453.

[9] C. Sullivan and A. Kaszynski. "PyVista: 3D plotting and mesh analysis through a streamlined interface for the Visualization Toolkit (VTK)". In: *Journal of Open Source Software* 4.37 (May 2019), p. 1450. DOI: 10.21105/joss.01450.

[10] W. Schroeder, K. Martin, and B. Lorensen. *The visualization toolkit*. 2nd ed. Upper Saddle River, NJ: Prentice Hall PTR, 1998.

[11] J. Schneiders et al. "Intracranial Aneurysm Neck Size Overestimation with 3D Rotational Angiography: The Impact on Intra-Aneurysmal Hemodynamics Simulated with Computational Fluid Dynamics". In: *American Journal of Neuroradiology* 34.1 (Jan. 2013), pp. 121–128. DOI: 10.3174/ajnr.A3179.

[12] M. R. Levitt et al. "One way to get there". In: *Journal of NeuroInterventional Surgery* 13.5 (May 2021), pp. 401–402. DOI: 10.1136/neurintsurg-2021-017559.

[13] Y. Qiao et al. "Intracranial arterial wall imaging using three-dimensional high isotropic resolution black blood MRI at 3.0 Tesla". In: *Journal of Magnetic Resonance Imaging* 34.1 (July 2011), pp. 22–30. DOI: 10.1002/jmri.22592.

[14] R. L. Greenman et al. "An assessment of the sharpness of carotid artery tissue boundaries with acquisition voxel size and field strength". In: *Magnetic Resonance Imaging* 26.2 (Feb. 2008), pp. 246–253. DOI: 10.1016/j.mri.2007.06.004.

[15] B. Zhao et al. "Endovascular Coiling of Wide-Neck and Wide-Neck Bifurcation Aneurysms: A Systematic Review and Meta-Analysis". In: *American Journal of Neuroradiology* 37.9 (Sept. 2016), pp. 1700–1705. DOI: 10.3174/ajnr.A4834.

[16] B. K. Hendricks et al. "Wide-neck aneurysms: systematic review of the neurosurgical literature with a focus on definition and clinical implications". In: *Journal of Neurosurgery* 133.1 (July 2020), pp. 159–165. DOI: 10.3171/2019.3.JNS183160.

[17] D. Backes et al. "Patient- and Aneurysm-Specific Risk Factors for Intracranial Aneurysm Growth: A Systematic Review and Meta-Analysis". In: *Stroke* 47.4 (Apr. 2016), pp. 951–957. DOI: 10.1161/STROKEAHA.115.012162.

[18] E. Laaksamo et al. "Intracellular Signaling Pathways and Size, Shape, and Rupture History of Human Intracranial Aneurysms". In: *Neurosurgery* 70.6 (June 2012), pp. 1565–1573. DOI: 10.1227/NEU.0b013e31824c057e.

[19] P. Berg et al. "Does the DSA reconstruction kernel affect hemodynamic predictions in intracranial aneurysms? An analysis of geometry and blood flow variations". In: *Journal of NeuroInterventional Surgery* 10.3 (Mar. 2018), pp. 290–296. DOI: 10.1136/neurintsurg-2017-012996.

[20] B. O'Meara et al. "Benefit of a Sharp Computed Tomography Angiography Reconstruction Kernel for Improved Characterization of Intracranial Aneurysms". In: *Operative Neurosurgery* 10.1 (Mar. 2014), pp. 97–105. DOI: 10.1227/NEU.0000000000000167.

[21] R. Anxionnat et al. "Intracranial Aneurysms: Clinical Value of 3D Digital Subtraction Angiography in the Therapeutic Decision and Endovascular Treatment". In: *Radiology* 218.3 (Mar. 2001), pp. 799–808. DOI: 10.1148/radiology.218.3.r01mr09799.

[22] T. Sugahara et al. "Comparison of 2D and 3D Digital Subtraction Angiography in Evaluation of Intracranial Aneurysms". In: *American Journal of Neuroradiology* 23.9 (2002), pp. 1545–52.